Neurosurgical Focus

Neurosurg Focus 6 (3): Article 4, 1999

Postimaging brain distortion: magnitude, correlates, and impact on neuronavigation

Neil L. Dorward, F.R.C.S., Olaf Alberti, M.D., Binti Velani, B.Sc., Frans A. Gerritsen, Ph.D., William F. J. Harkness, F.R.C.S., Neil D. Kitchen, F.R.C.S., and David G. T. Thomas, F.R.C.P., F.R.C.S.

Gough-Cooper Department of Neurological Surgery, Institute of Neurology, London, United Kingdom; Department of Surgical Neurology, National Hospital for Neurology and Neurosurgery, London, United Kingdom; and Integrated Clinical Solutions, Philips Medical Systems B.V., Best, The Netherlands

This prospective study was conducted to quantify brain shifts during open cranial surgery, to determine correlations between these shifts and image characteristics, and to assess the impact of postimaging brain distortion on neuronavigation.

During 48 operations, movements of the cortex on opening, the deep tumor margin, and the cortex at completion were measured relative to the preoperative image position with the aid of an image-guidance system. Bone surface offset was used to assess system accuracy and correct for registration errors. Preoperative images were examined for the presence of edema and to determine tumor volume, midline shift, and depth of the lesion below the skin surface. Results were analyzed for all cases together and separately for four tumor groups: 13 meningiomas, 18 gliomas, 11 nonglial intraaxial lesions, and six skull base lesions.

For all 48 cases the mean shift of the cortex after dural opening was 4.6 mm, shift of the deep tumor margin was 5.1 mm, and shift of the cortex at completion was 6.7 mm. Each tumor group displayed unique patterns of shift, with significantly greater shift at depth in meningiomas than gliomas ($p = 0.007$) and significantly less shift in skull base cases than other groups ($p < 0.003$). Whereas the preoperative image characteristics correlating with shift of the cortex on opening were the presence of edema and depth of the tumor below skin surface, predictors of shift at depth were the presence of edema, the lesion volume, midline shift, and magnitude of shift of the cortex on opening.

This study quantified intraoperative brain distortion, determined the different behavior of tumors in four pathological groups, and identified preoperative predictors of shift with which the reliability of neuronavigation may be estimated.

Key Words * brain shift * computer-assisted surgery * interactive image-guided surgery * neuronavigation * postimaging brain distortion

Brain distortion is an everyday experience for the neurosurgeon; it is concomitant with the practice of neurosurgery and the occurrence of this phenomenon is not disputed. However, the magnitude of such distortion, the influence of tumor type, and the imaging characteristics that predict shift are poorly understood. Furthermore, the impact of brain shift on image guidance, the need for intraoperative image updating, and the resolution necessary for such updating are controversial and unresolved issues.[1,3,6,9,12] To resolve these controversies requires knowledge of the magnitude, directions, influences, and predictors of postimaging brain distortion, information that is currently unavailable in the literature.

We report the results of a prospective study designed to quantify postimaging brain distortion, demonstrate variations between tumor groups, and identify predictors of shift in relation to preoperative images. Movement of the cortical surface on dural opening, the deep tumor margin, and the cortical surface at completion were measured and imaging characteristics were identified that correlated with these shifts. The findings are discussed in relation to the impact of postimaging brain distortion on the reliability of neuronavigation for different surgically treated tumors and for the prediction of error in individual cases.

CLINICAL MATERIAL AND METHODS

Patient Population

During the period between June 1996 and April 1997 a total of 93 image-guided operations were performed at our institution. The male/female ratio of the patients in whom these operations were performed was 1.5:1 and the mean age was 44.7 years (Table 1). Cases were selected on the basis of a request for navigational guidance from the operating surgeon. Three of the selected patients did not undergo image-guided surgery; one was unable to undergo magnetic resonance (MR) imaging because of a ferrous implant, one was confused and removed all skin fiducials between the time of scanning and surgery, and one died the night before surgery. Brain shift measurements and bone surface localization errors were obtained in 48 of the 93 image-guided cases. Shift measurements were not obtained in the remaining 45 cases for a variety of reasons. Burr hole biopsy and shunt procedures were necessarily excluded from the study because measurement of shift at depth was not feasible in such cases. In other cases data acquisition was precluded by surgical time constraints, poorly demarcated lesion margins, and in two cases loss of registration prior to completion. The mean age of the 48 patients in the study group was 47.1 years and the male/female ratio was 1:1 (Table 1).

TABLE 1
COMPARISON OF THE STUDY GROUP AND ALL PATIENTS UNDERGOING IMAGE-GUIDED SURGERY*

Characteristic	All Patients	Study Group
no. of cases	93	48
male/female ratio	1.5:1	1:1
mean age (range)	47 (15–77)	47.1 (20–77)
mean registration RMSE	3.6 (SD 1.1)	3.6 (SD 1)
pathological group (%)		
I	20 (21)	13 (27)
II	27 (29)	18 (38)
III	25 (27)	11 (23)
IV	21 (23)	6 (12)

* No statistical difference was found between these groups.

There were no statistically significant differences between the study subgroup and the total patient population (that is, the study subgroup was accurately representative of our normal patient population). The tumors were divided into four groups for data analysis: Group I, convexity and parasagittal meningiomas; Group II, cerebral gliomas; Group III, nonglial intraaxial lesions; and Group IV, skull base lesions (Table 2).

TABLE 2

BREAKDOWN OF THE STUDY GROUP ACCORDING TO HISTOLOGICAL DIAGNOSIS OF LESIONS AND ALLOCATION TO TUMOR GROUPS FOR DATA ANALYSIS*

Tumor Group	Histological Diagnosis	No. of Tumors
I: vault meningiomas	meningioma	13
II: cerebral gliomas	glioma	18
III: nonglial intraaxial lesions	colloid cyst of third ventricle	2
	metastasis	1
	hemangioblastoma	1
	DNET	1
	choroid plexus papilloma	1
	ependymoma	1
	cavernoma	1
	granuloma	1
	abscess	1
	epileptic focus	1
IV: skull base lesions	meningioma	2
	chordoma	1
	neurilemmoma	1
	epidermoid	1
	arachnoid cyst	1

* DNET = dysembryoblastic neuroepithelial tumor.

Preoperative Imaging and Image Analysis

All patients underwent preoperative studies consisting of gadolinium-enhanced T_1-weighted volumetric MR imaging in which the adhesive multimodality surface fiducial markers remained in situ. Two machines were used: a 1.5-tesla Signa (General Electric Inc., Milwaukee, WI) and a 0.5-tesla Vectra scanner (General Electric Inc.). The imaging protocols were TR 14.2, TE 3.3, flip angle 30š, matrix 256 X 256, field of view 24 cm, thickness 160 mm; and TR 45, TE 15, flip angle 50š, matrix 192 X 192, field of view 24 cm, thickness 180 mm, respectively. The resultant voxel sizes in millimeters were X = 0.93, Y = 0.93, and Z = 1.30 for the Signa apparatus and X = 1.25, Y = 1.25, and Z = 2.25 for the Vectra. All image data sets were transferred via ethernet to an image-processing workstation (EasyVision CT/MR; Philips Medical Systems B.V., Best, The Netherlands) for evaluation. In each case the maximum midline shift, lesion volume, depth of the lesion below the skin surface, and presence or absence of edema were determined. Depth and volume were measured by first finding the center of the lesion in the standard three orthogonal views. Distance from this center of density to the nearest skin surface was then measured in millimeters by using a software caliper tool. The three perpendicular radii (X, Y, and Z) of the lesion were then found from the measurement of diameters bisecting this central point: in the anteroposterior plane on the axial view (a), the left to right diameter in the coronal plane (b), and the cephalocaudal diameter on the sagittal view (c). Lesion volume was calculated from these measurements using the formula for the volume of an ellipsoid (volume = 4/3 ¼$r_a r_b r_c$). Midline shift was determined as the maximum diversion of the midline from a line joining the anterior and posterior origins of the falx

cerebri in the axial plane.

Neuronavigation Technique

The navigation system used for this study (EasyGuide Neuro; Philips Medical Systems B.V.) comprised a table-mounted array incorporating two infrared cameras, a mobile computer workstation with a high-resolution monitor, and handheld pointers with infrared light-emitting diodes.[5,18] The MR imaging data sets were transferred to the operating system via ethernet or optical disk, and the position of each fiducial marker was selected manually. After patient positioning and application of the Mayfield head clamp (OMI Surgical Products, Cincinnati, OH) patient-to-image registration was performed using a nonsterile handheld pointer. After registration, axial, coronal, and sagittal reconstructions of the pointer tip position were displayed in real time on the monitor. Software tools for virtual pointer elongation, path planning, and caliper measurement were used, and the system-derived root mean square error (RMSE) of registration fit was recorded in each case.

Brain Shift Measurement Technique

The structures examined in this study were the skull surface at the center of the planned craniotomy, the cortical surface at the center of the dural opening (or, in the case of meningiomas, the most central cortex adjacent to the tumor), the deep tumor margin, and the cortical surface adjacent to the resection margin at completion. To detect and measure postimaging brain distortion, the surgeon first identified the required surface and gently touched a sterile handheld light-emitting diode pointer to this structure. The position of the pointer tip was automatically displayed in the preoperative images on the system monitor. When shift was present the pointer tip position appeared to lie at a distance from the chosen structure in the images. The system was then temporarily inactivated while this distance was measured with the caliper tool (Fig. 1) in each of the views in which the surface was visible. Measurement of shift of the deep tumor margin was only undertaken when the surgeon could identify this structure with confidence.

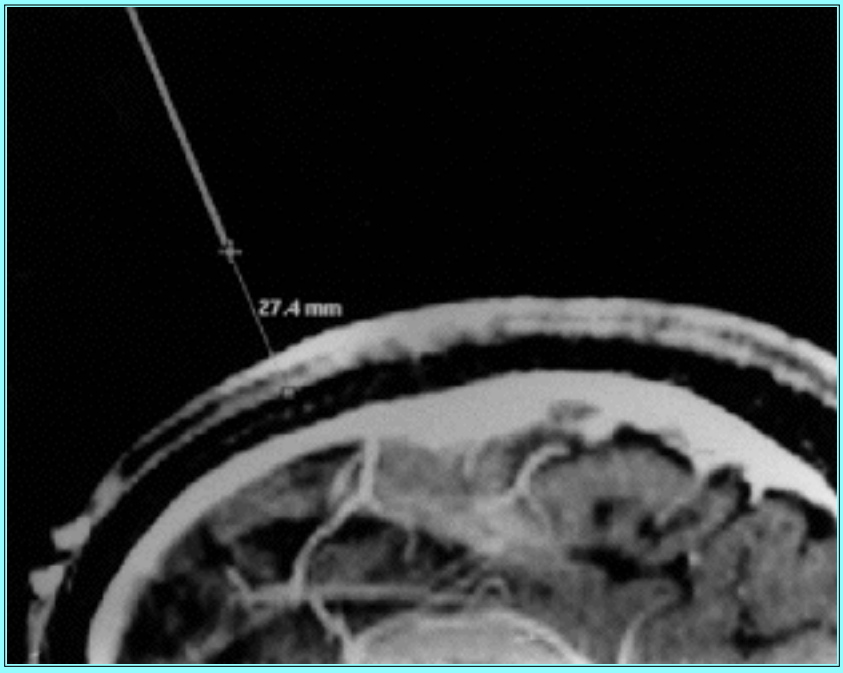

Fig. 1. Photograph of the neuronavigation system's screen demonstrating the method of distortion measurement. The distance between the pointer tip, which is placed on the bone surface in this example, and the bone surface in the preoperative images is determined with

the caliper tool (the distance has been exaggerated for clarity).

Statistical Analysis

Measurements were assigned positive or negative values according to the direction of shift: positive for outward bulging and negative for infalling. The brain shift measurements in each case were corrected for registration skew by the subtraction of the bone surface offset respective of sign. This method presumes that translational mismatching of image coordinates with operating area coordinates will apply to each of the surfaces equally across a small area. The resultant data were analyzed for patterns, correlations, and significance as a whole and then segregated according to tumor groups. The statistical tests of significance used were the unpaired two-tailed t-tests for normally distributed data and chi-square tests for noncontinuous data (significance established at $p < 0.05$). Correlations were accepted when the sample correlation coefficient value exceeded 0.4 and the associated probability value was less than 0.05.

RESULTS

Preoperative Image Analysis

Examination of the values for lesion volume, midline shift, distance below skin surface, and incidence of edema (Table 3) determined from the preoperative MR studies allowed us to identify patterns particular to each tumor group (Fig. 2). Comparison of groups revealed that the mean volume of Group III tumors was significantly less than that found in the other lesions ($p = 0.021$). The extent of midline shift was significantly greater in Group I than in the other groups ($p = 0.031$) and significantly lower in Group III than in the other groups ($p = 0.011$). The mean distance below the skin surface was, not surprisingly, significantly less for tumors in Group I than for those in the other groups ($p = 0.0007$). Similarly, the frequency of reactive edema was significantly greater in Group I than in Group II ($p < 0.02$) and all other groups ($p < 0.001$).

TABLE 3

PREOPERATIVE IMAGING CHARACTERISTICS FOR ALL 48 PATIENTS STUDIED AND BREAKDOWN ACCORDING TO TUMOR GROUP

Imaging Characteristic	All (48 patients)	Group I (13 patients)	Group II (18 patients)	Group III (11 patients)	Group IV (6 patients)
volume (ml)	24.5	34.4	26.8	9.6	23.6
range	0.6–140.5	5.3–76.4	0.9–140.5	0.6–40.3	4.7–47.5
SD	26.7	21.3	34.9	11.9	20.1
midline shift (mm)	4.5	7.5	4.4	2.1	3.6
range	0–19.9	1.8–19.9	0.0–12.9	0.0–7.6	0.0–8.3
SD	4.5	5.3	4.5	2.8	2.8
depth below skin (mm)	40.5	31.3	36.5	53.3	49.5
range	14.1–71.9	14.1–43.6	23.8–53.3	22.9–71.9	21.1–66.1
SD	14.5	8.6	9.4	15.7	16.6
percentage w/ edema	60	100	67	36	17

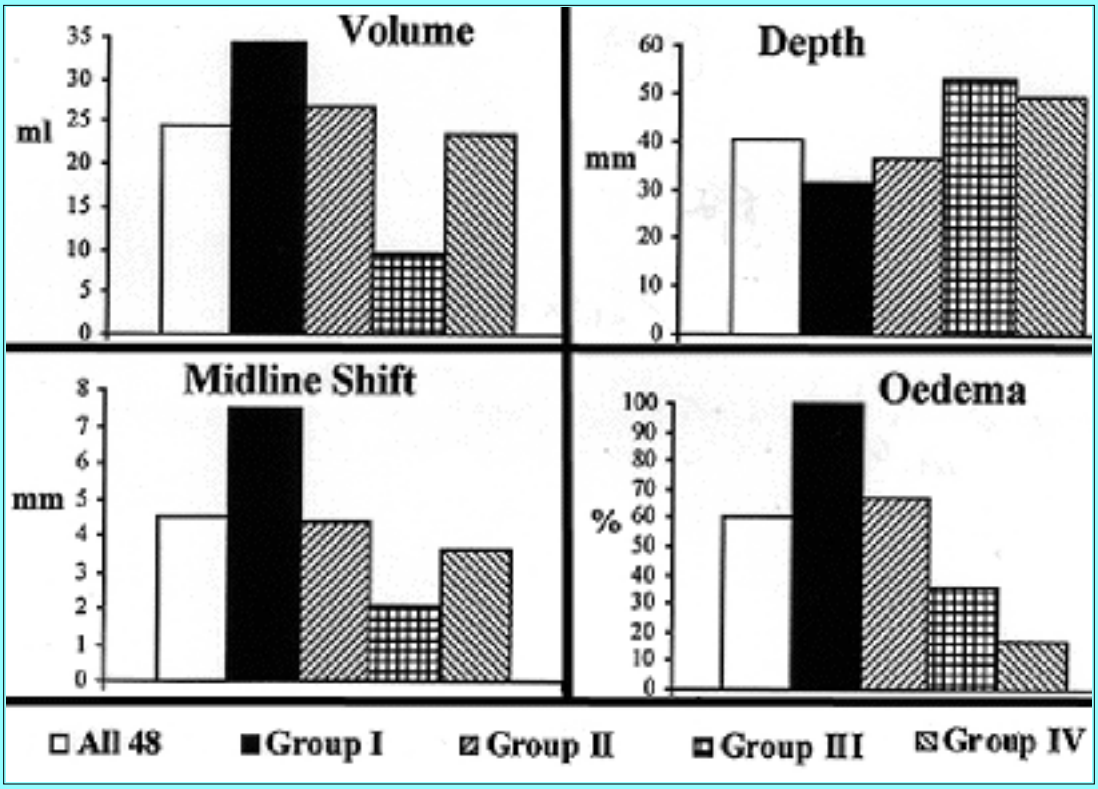

Fig. 2. Bar graphs displaying preoperative MR imaging characteristics according to tumor group. The occurrence of reactive edema is given as the percentage of tumors with edema present.

Neuronavigation System Accuracy

Laboratory phantom studies and in vivo accuracy assessments have shown the errors associated with clinical application of mechanical arm-based systems to be approximately 2.5 to 3 mm[20,21] and of optical systems to be 2 mm or less for the majority of cases,[9,22] comparing well with the accuracy of frame-based systems.[17] The accuracy of tracking with the neuronavigation system used in this report as assessed in phantom studies has been calculated as 0.66 mm for 3-mm slices on computerized tomography scans[8] and the mean bone surface offset (registration error) in this study was 2.1 mm (median 1.7 mm, standard deviation [SD] 2). The system-derived RMSE of patient-to-image registration was 3.6 mm (median 3.5 mm, SD 1).

Magnitude of Postimaging Brain Distortion

The mean corrected shift of the cortex on opening for all 48 cases was 4.6 mm (0.0-20.4, SD 4), the mean shift of the deep tumor margin was 5.1 mm (0.0-24.2, SD 5.8), and the mean cortex shift at completion was 6.7 mm (0.0-19.9, SD 5.7) (Table 4).

TABLE 4

MAGNITUDE OF BRAIN SHIFT FOR ALL 48 PATIENTS STUDIED AND BREAKDOWN ACCORDING TO TUMOR GROUP*

Imaging Characteristic	All (48 patients)	Group I (13 patients)	Group II (18 patients)	Group III (11 patients)	Group IV (6 patients)
shift of cortex on opening	4.6	4.3	5.8	3.7	2.0
range	0.0–20.4	0.4–12.1	0.0–20.4	0.3–10.1	1.0–3.6
SD	4.0	3.2	5.1	2.9	1.4
shift of deep tumor margin	5.1	10.0	3.5	2.4	1.2
range	0.0–24.2	0.8–24.2	0.0–13.7	0.1–12.1	0.0–3.4
SD	5.8	6.5	4.2	4.3	1.5
shift of cortex at completion	6.7	9.4	4.2	9.4	1.1
range	0.0–19.9	0.6–19.9	0.0–10.5	3.4–16.2	0.0–3.9
SD	5.7	6.9	3.0	4.8	1.9

* All values are expressed as millimeters.

Thus the overall magnitude of postimaging brain distortion was seen to rise as the operations proceeded. However, starkly different patterns were revealed when the shift data were analyzed separately for each tumor group (Fig. 3).

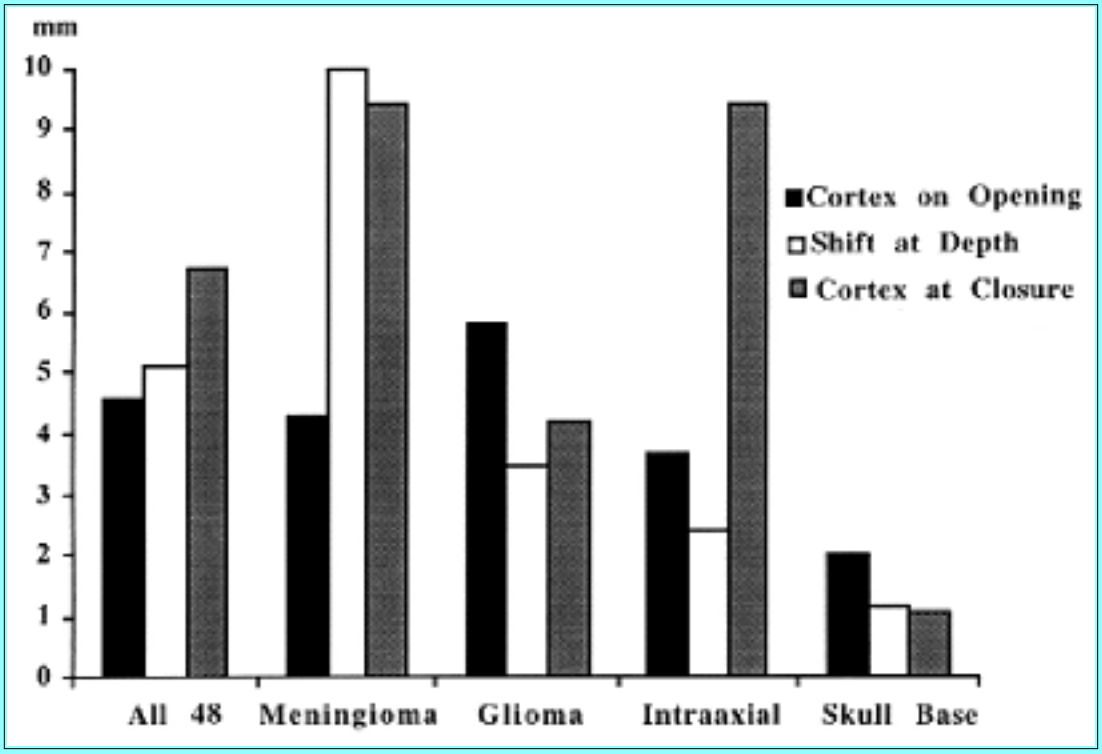

Fig. 3. Bar graph of mean brain shift according to tumor group, demonstrating the different patterns of shift revealed by the study.

In Group I, the shift of the deep tumor margin was the greatest of all shifts (mean = 10 mm), and shift was significantly greater (Table 5) than both deep shifts in other groups ($p = 0.0032$) and shift of the cortex on opening in Group I ($p = 0.015$). Also in Group I, shift of the cortex at completion was significantly greater than that found on opening ($p = 0.041$). In Group II shift of the deep tumor margin and shift of the cortex at completion were both lower than cortical shift on opening. In Group III cortical

shift on opening and shift at depth were significantly lower than shift of the cortex at completion (p = 0.014 and p = 0.012, respectively). In Group IV shift at depth and shift of the cortex at completion were significantly lower than in other groups (p = 0.003 and p = 0.0006, respectively).

TABLE 5

STATISTICALLY SIGNIFICANT DIFFERENCES BETWEEN THE MAGNITUDE OF BRAIN SHIFT WITHIN AND BETWEEN TUMOR GROUPS

Tumor Group & Larger Variable	Tumor Group & Smaller Variable	p Value
I & shift at depth	II & shift at depth	0.007
I & shift at depth	all others & shift at depth	0.0032
I & cortex shift at completion	II & cortex shift at completion	0.04
all others & cortex shift on opening	IV & cortex shift on opening	0.047
all others & shift at depth	IV & shift at depth	0.003
all others & cortex shift at completion	IV & cortex shift at completion	0.0006
III & cortex shift at completion	III & cortex shift on opening	0.014
III & cortex shift at completion	III & shift at depth	0.012
I & shift at depth	I & cortex shift on opening	0.015
I & cortex shift at completion	I & cortex shift on opening	0.041

Direction of Brain Shifts

The direction of shift at each stage of surgery (outward bulging or infalling) also showed striking differences between tumor groups. The pattern for all 48 cases was outward bulging of the cortex on opening in 67%, infalling in 30%, and level in 3% (Fig. 4). At the tumor bed there was an outward shift in 72%, infalling in 23%, and no shift in 5%. At completion the direction of cortex shift was bulging in 26%, infalling in 69%, and level in 5%. Tumor groups again showed marked differences in the pattern of direction of shifts at each stage. Thus, in Group I the same pattern was exaggerated, with bulging in 73% of cases at opening, bulging in 100% at the deepest tumor margin, and infalling of the cortex in 82% at completion. In Groups II and III the pattern was similar to that for all 48 cases together, and in Group IV, with the smallest recorded shifts, infalling of the cortex at opening was seen in the majority, minimal bulging at depth, and slight infalling at completion.

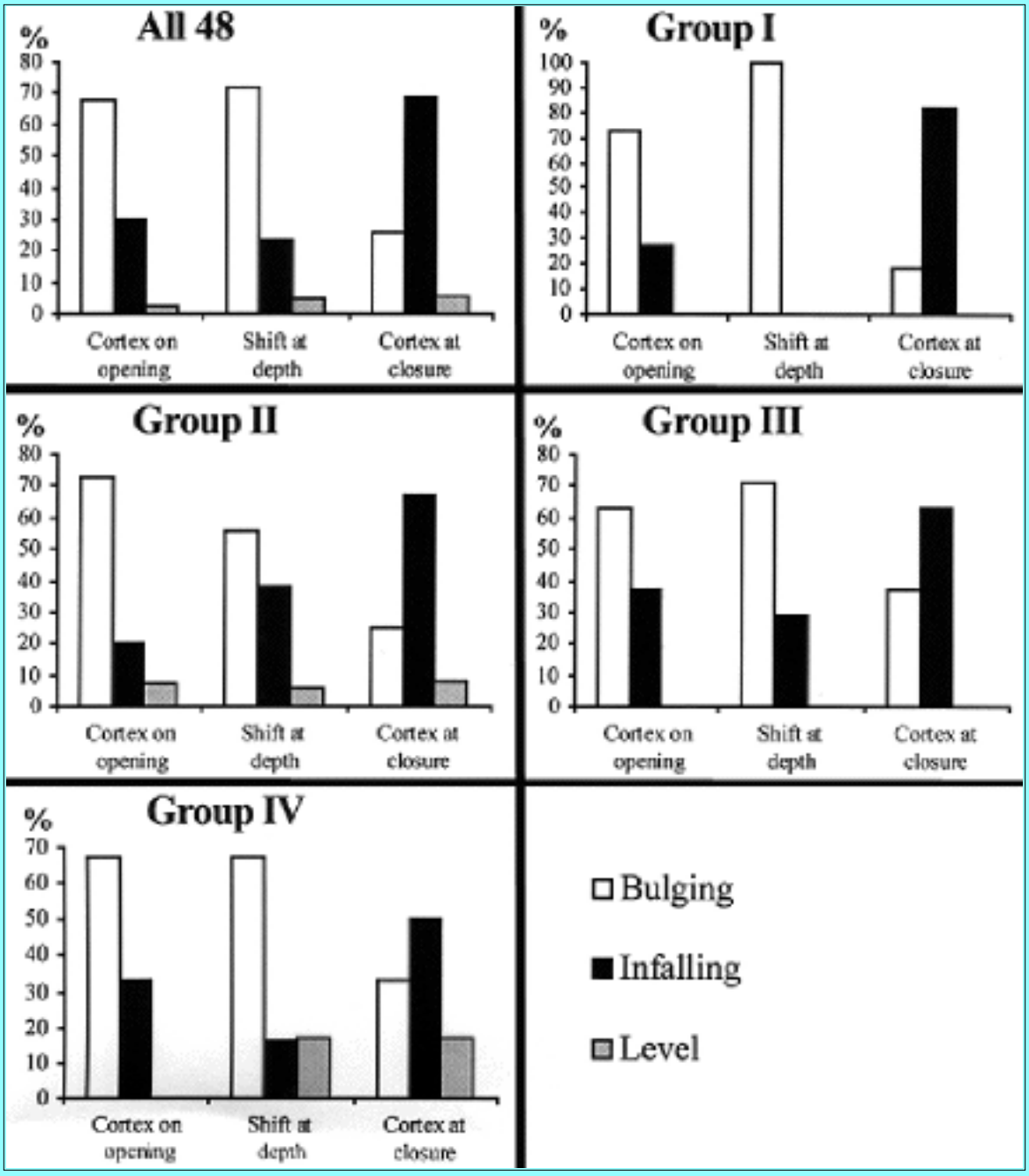

Fig. 4. Bar graphs displaying the direction of brain shift on opening, at depth, and at completion (closure) for each tumor group.

Correlations Between Variables

Analysis of preoperative image characteristics and brain shift measurements revealed a number of correlations that had statistical significance. For all 48 cases together, shift of the cortex on opening was negatively correlated with distance of the lesion below the skin surface ($r = -0.41$, $p = 0.012$) and was positively correlated with the presence of edema ($p = 0.013$). Shift of the deepest tumor margin was positively correlated with lesion volume ($r = 0.51$, $p = 0.001$), midline shift ($r = 0.52$, $p = 0.001$), and the presence of edema ($p = 0.035$). When each group was analyzed individually, further correlations were revealed. In Group I, shift of the cortex at completion was positively correlated with tumor volume ($r = 0.61$, $p = 0.046$) and midline shift ($r = 0.64$, $p = 0.045$) and negatively correlated with distance below the skin surface ($r = -0.69$, $p = 0.018$). In Group II, shift of the cortex on opening was positively correlated with midline shift ($r = 0.53$, $p = 0.043$) and negatively correlated with distance below the skin surface (r

= -0.55, p = 0.033), whereas shift at depth was positively correlated with midline shift (r = 0.56, p = 0.024) and tumor volume (r = 0.68, p = 0.004). In Group III, shift of the cortex on opening and shift at depth showed a strong positive correlation with tumor volume (r = 0.8, p = 0.017 and r = 0.94, p = 0.002, respectively), and shift of the cortex at completion was positively correlated with midline shift (r = 0.8, p = 0.017). Additionally, when the relationships between each of the shift parameters were examined, shift of cortex on opening was found to be positively correlated with shift at the deepest tumor margin (r = 0.5, p = 0.006) for all 48 cases and for individual tumor groups (Fig. 5).

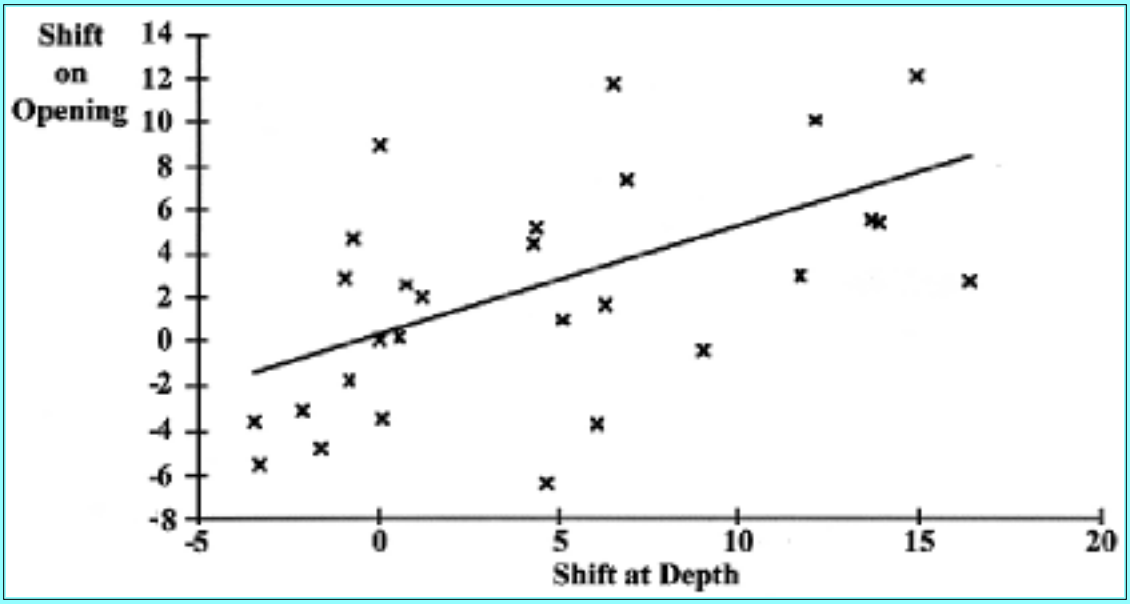

Fig. 5. Scatterplot and linear regression illustrating the correlation between shift of the cortex on opening and shift of the deepest tumor margin (r = 0.5, p = 0.006).

DISCUSSION

Interactive image guidance is an increasingly important tool in neurosurgery.[7] Reported benefits include an improved surgical approach,[2,3,19] reduced morbidity rates,[19] shorter hospital stay,[10,19] reduced hospital costs,[10,19] and reduced requirements for postoperative analgesia.[3] However, the provision of reliably accurate guidance requires both low system error and a high rate of congruence between preoperative images and surgical anatomy. Although the errors associated with image acquisition, registration, and tracking have been defined,[8,9,16,18-20,22] the magnitude and impact of postimaging brain distortion on this congruence is poorly understood. The causes of postimaging brain distortion are likely to be both physiological and physical. Physiological factors include therapeutic and incidental manipulations of total and cerebral blood volume, administration of diuretic medications, and mechanical ventilation. Although the effects of such manipulations on intracranial pressure have been extensively studied, the specific effect on gray matter, white matter, cerebrospinal fluid, tumor, and edematous brain volumes is not clear. Also, differential effects on these tissues would inevitably lead to complex postimaging brain distortion rather than simple total brain volume changes. The major physical factors that give rise to brain distortion are likely to be pressure changes on skull opening, unopposed gravity, patient positioning, cerebrospinal fluid withdrawal, ventricular compression, retraction, and tissue removal. However, none of these is well understood or extensively researched.

Although perioperative brain distortion has often been noted to occur,[6,9,21] the critical issues of the magnitude of such shifts, changes with depth, and impact on neuronavigation have not been addressed. Despite this, concern about the effects of postimaging brain distortion on the accuracy of image guidance

has prompted the development of elaborate methods to circumvent this perceived problem. These include insertion of ball bearings[11] or catheters to correct for shifts during resection and image updating with ultrasonography,[4,13] computerized tomography,[14,15] and interventional MR imaging. In this study we have determined the magnitude of, patterns in, and influences on postoperative brain distortion and have assessed their true impact on the accuracy of image-guided surgery according to each tumor group.

Group I

The patients in this group displayed relatively consistent group-specific patterns of brain distortion that can be exploited. Thus, shift of the cortex on opening was modest whereas shift at depth and cortex at completion were significantly greater than in other groups. The direction of shift also followed a consistent pattern in meningiomas, with bulging on opening, bulging at the deepest tumor margin, and infalling at completion in the majority of cases. The implication for image guidance is that during meningioma surgery, flap positioning and tumor margin delineation can be relied on, but the deep tumor margin will be elevated toward the surgeon and encountered sooner than indicated on the image-guidance system. However, it should be noted that in this group the deep tumor margin represents compressed cortical tissue and that our method of measuring tumor bed shift after removal may overestimate the shift during resection, when the bulging of normal brain is inhibited by the presence of residual tumor.

Group II

Gliomas exemplify the desirability of accurate image guidance at depth when tumor margins are poorly demarcated, maximum removal is desired, and eloquent brain areas abut the lesion. Fortunately, the pattern of shifts revealed during glioma surgery by this study complement the role of neuronavigation. Thus, shift of the deepest tumor margin was significantly less in gliomas than that seen in meningiomas and was less than the shift of cortex on opening and at completion within Group II. In addition, correlations were identified between the preoperative image measures of tumor volume and midline shift and the magnitude of shift at depth. The implication for neuronavigation in glioma surgery is that image-guided resection is feasible and reliable but should be used with caution when preoperative images reveal a particularly large mass with marked deviation of the midline.

Group III

These lesions were significantly smaller, produced significantly less midline shift, and provoked less edema than those of other groups. Therefore, it is not surprising that the shift at depth in this group was significantly less than in the other groups. However, despite both the small mean size and the low associated shifts, there was a strong correlation between tumor volume and shift at depth. The implication is that postimaging distortion is slight, is smallest at depth, and that image guidance should be highly reliable. In addition, reduced accuracy may be predicted if the lesion is unusually large on the preoperative MR image.

Group IV

These lesions are remarkable for the low incidence of edema and the small magnitude of each shift (both significantly less than in all other groups). These factors predict good reliability for neuronavigation in the treatment of skull base lesions.

General Implications for Neuronavigation

The magnitude of brain shifts recorded in this study are not perceived to negate the value of image guidance in the majority of cases, and the predictive factors identified here should allow cases accompanied by above-average shift to be identified preoperatively. Naturally, care must be taken in extrapolating such data to other patient populations. For example, in our institution it is not a routine practice to administer mannitol, operations are not generally longer than 2 to 3 hours in duration, and many tumors are of a considerable size. We hope that these findings will stimulate further investigations into the nature of postimaging brain distortion and assist in the appropriate application and design of intraoperative image-updating methods.

CONCLUSIONS

We regard these findings as robust evidence for the value and reliability of neuronavigation. We conclude that measurable brain shift occurs during open cranial surgery, that guidance of deep resection of intrinsic lesions is possible, and that above-average shifts can be predicted from preoperative images. Image guidance should be used with caution at the deep margin of superficial extrinsic tumors. We suggest that additional work based on further quantitative studies is needed to identify means to control or correct for these shifts in individual cases and to improve the usefulness of neuronavigation further.

Acknowledgments

This research was performed within the context of the European Applications for Surgical Interventions (EASI) project, supported by the European Commission in their "4th Framework Telematics Applications for Health" Research and Technological Development program. The partners in the EASI consortium are: The National Hospital for Neurology and Neurosurgery in London, United Kingdom; the Laboratory for Medical Imaging Research of the Katholieke Universiteit in Leuven, Belgium; the Image Sciences Institute of Utrecht University and University Hospital in Utrecht, The Netherlands; Philips Medical Systems Nederland B.V., in Best, The Netherlands; Philips Research Laboratory in Hamburg, Germany; and the Image Processing Group of Radiological Sciences at the United Medical and Dental Schools of Guy's and St. Thomas' Hospitals in London, United Kingdom.

References

1. Barnett GH, Kormos DW, Steiner CP, et al: Use of a frameless, armless stereotactic wand for brain tumor localization with two-dimensional and three-dimensional neuroimaging. **Neurosurgery 33:**674-678, 1993

2. Barnett GH, Steiner CP, Weisenberger J: Intracranial meningioma resection using frameless stereotaxy. **J Image Guided Surg 1:**46-52, 1995

3. Bucholz RD, Smith KR: A comparison of sonic digitizers versus light emitting diode-based localization, in Maciunas RJ (ed): **Interactive Image-Guided Neurosurgery.** Park Ridge, Ill: American Association of Neurological Surgeons, 1993, pp 179-200

4. Bucholz R, Sturm C, Henderson J: Detection of brain shift with an image guided ultrasound device. **Acta Neurochir 138:**627, 1996 (Abstract)

5. Buurman J, Gerritsen FA: European Applications in Surgical Interventions (EASI), in Lemke HU, Vannier MW, Inamura K, et al (eds): **CAR '96. Computer Assisted Radiology.** Amsterdam: Elsevier,

1996 pp 677-685

6. Drake JM, Rutka JT, Hoffman HJ: ISG viewing wand system. **Neurosurgery 34:**1094-1097, 1994

7. Dorward NL: Neuronavigation--the surgeon's sextant. **Br J Neurosurg 11:**101-103, 1997

8. Fuchs M, Wischmann HA, Neumann A, et al: Accuracy analysis for image-guided neurosurgery using fiducial skin markers, 3D CT imaging and an optical localizer system, in Lemke HU, Vannier MW, Inamura K, et al (eds): **CAR '96. Computer Assisted Radiology.** Amsterdam: Elsevier, 1996, pp 770-775

9. Golfinos JG, Fitzpatrick BC, Smith LR, et al: Clinical use of a frameless stereotactic arm: results of 325 cases. **J Neurosurg 83:**197-205, 1995

10. Henderson JM, Eichholz KM, Bucholz RD: Decreased length of stay and hospital costs in patients undergoing image-guided craniotomies. **J Neurosurg 86:**367A, 1997 (Abstract)

11. Kelly PJ: Stereotactic excision of brain tumours, in Thomas DGT (ed): **Stereotactic and Image Directed Surgery of Brain Tumours.** Edinburgh: Churchill Livingstone, 1993, pp 89-109

12. Kelly PJ, Kall BA, Goerss SJ: Results of computed tomography-based computer-assisted stereotactic resection of metastatic intracranial tumors. **Neurosurgery 22:**7-17, 1988

13. Koivukangas J, Louhisalmi Y, Alakuijala J, et al: Ultrasound-controlled neuronavigator-guided brain surgery. **J Neurosurg 79:**36-42, 1993

14. Kwoh YS, Hou J, Jonckheere EA, et al: A robot with improved absolute positioning accuracy for CT guided stereotactic brain surgery. **IEEE Trans Biomed Eng 35:**153-160, 1988

15. Lunsford LD, Kondziolka D, Bissonette DJ: Intraoperative imaging of the brain. **Stereotact Funct Neurosurg 66:**58-64, 1996

16. Maciunas RJ (ed): **Interactive Image-Guided Neurosurgery.** Park Ridge, Ill: American Association of Neurological Surgeons, 1993

17. Maciunas RJ, Galloway RL Jr, Latimer J, et al: An independent application accuracy evaluation of stereotactic frame systems. **Stereotact Funct Neurosurg 58:**103-107, 1992

18. Rohling R, Munger P, Hollerbach JM, et al: Comparison of accuracy between a mechanical and an optical tracker for image-guided neurosurgery. **J Image Guided Surg 1:**30-34, 1995

19. Sandeman DR, Patel N, Chandler C, et al: Advances in image-directed neurosurgery: preliminary experience with the ISG Viewing Wand compared with the Leksell G frame. **Br J Neurosurg 8:**529-544, 1994

20. Sipos EP, Tebo SA, Zinreich SJ, et al: In vivo accuracy testing and clinical experience with the ISG Viewing Wand. **Neurosurgery 39:**194-202, 1996

21. Spetzger U, Laborde G, Gilsbach JM: Frameless neuronavigation in modern neurosurgery. **Minim Invasive Neurosurg 38:**163-166, 1995

22. Vrionis FD, Foley KT, Robertson JH, et al: Use of cranial surface anatomical fiducials for interactive

image-guided navigation in the temporal bone: a cadaveric study. **Neurosurgery 40:**755-764, 1997

Manuscript received July 29, 1997.

Accepted in final form November 11, 1997.

This research was supported by a Grant No. HC1012 from the European Commission as part of the EASI project.

Address reprint requests to: Neil L. Dorward, F.R.C.S., Gough-Cooper Department of Neurological Surgery, National Hospital For Neurology and Neurosurgery, Queen Square, London WC1N 3BG, United Kingdom.
